Наносистеми, наноматеріали, нанотехнології
Nanosistemi, Nanomateriali, Nanotehnologii
2016, т. 14, № 3, сс. 435–444

PACS numbers: 82.45.Aa, 82.45.Fk, 82.45.Yz, 82.47.Jk, 82.47.Uv, 82.47.Wx, 84.32.Tt

High-Performance Electrode Based on Activated Carbon for Electrochemical Energy Sources

B. P. Bakhmatyuk, I. Ya. Dupliak, and J. M. Voitovic

Lviv Polytechnic National University,
Department of Applied Physics and Nanomaterials Science,
12 Stepan Bandera Str.,
79013 Lviv, Ukraine

This study shows that 'Norit DLC Supra 30' commercial activated carbon material (NS commercial ACM) provides high-performance electrode for electrochemical energy sources (EES) in 25% ZnI_2 aqueous electrolyte. This is shown on the basis of the analysis of the desorption isotherms of iodine, the dependences of the specific discharge capacity (C_d) on current load, and the Ragone plot drawn using galvanostatic charge–discharge (GCD) dependences at a current density (i) range of 0.5–9 $A \cdot g^{-1}$. High values of fractional surface coverage (θ), from 0.73 to 0.87, determine large values of specific energy (W), from 1240 $J \cdot g^{-1}$ to 1096 $J \cdot g^{-1}$, at the values of specific power (P) range from 0.6 to 8 $W \cdot g^{-1}$. NS commercial ACM shows high values of specific energy ($W = 1217$ $J \cdot g^{-1}$), specific capacitance ($C_d = 1156$ $C \cdot g^{-1}$), Coulomb efficiency ($\eta = 88\%$), and specific power ($P = 4.3$ $W \cdot g^{-1}$) in the 2000^{th} cycle.

Це дослідження показує, що комерційний активований вуглецевий матеріал "Norit DLC Supra 30" забезпечує електроду з високими показниками для електрохемічних енергетичних джерел у 25%-водному електроліті ZnI_2. Це показано на основі аналізи ізотерм десорбції йоду, залежностей питомої розрядної ємности від струмового навантаження, а також Раґонового графіка, нарисованого з використанням ґальваностатичних заряд–розряд-залежностей при діяпазоні густини електричного струму 0,5–9 А/г. Високі значення ступеня поверхневого покриття від 0,73 до 0,87 визначають великі значення питомої енергії від 1240 Дж/г до 1096 Дж/г при значеннях діяпазону питомої потужности від 0,6 до 8 Вт/г. Комерційний активований вуглецевий матеріял "Norit DLC Supra 30" демонструє високі значення питомої енергії (1217 Дж/г), питомої ємности (1156 К/г), Кулонової ефективности (88%), а також питомої потужности (4,3 Вт/г) у 2000-у циклі.

Это исследование показывает, что коммерческий активированный угле-

родный материал «Norit DLC Supra 30» обеспечивает электрод с высокими показателями для электрохимических энергетических источников в 25%-водном электролите ZnI_2. Это показано на основе анализа изотерм десорбции йода, зависимостей удельной разрядной ёмкости от токовой нагрузки, а также рагоновского графика, нарисованного с использованием гальваностатических заряд–разряд-зависимостей при диапазоне плотности электрического тока 0,5–9 А/г. Высокие значения степени поверхностного покрытия от 0,73 до 0,87 определяют большие значения удельной энергии от 1240 Дж/г до 1096 Дж/г при значениях диапазона удельной мощности от 0,6 до 8 Вт/г. Коммерческий активированный углеродный материал «Norit DLC Supra 30» демонстрирует высокие значения удельной энергии (1217 Дж/г), удельной ёмкости (1156 К/г), кулоновской эффективности (88%), а также удельной мощности (4,3 Вт/г) в 2000-м цикле.

Key words: Ragone plot, capacity, cycling life.

Ключові слова: Раґонів графік, ємність, гранична кількість циклів служби.

Ключевые слова: рагоновский график, ёмкость, предельное количество циклов службы.

(Received 4 September, 2016)

1. INTRODUCTION

Due to environmental friendliness, low cost, high corrosion resistance, good electrical conductivity, and a highly porous structure, activated carbon materials remain the most attractive and accessible materials for electric double layer capacitors [1–4]. Alongside with oxides and nitrides of metals, conductive polymers, ACM are used for electrosorption of hydrogen and iodine in asymmetric systems of electrochemical supercapacitors and as positive electrode in lithium-ion capacitors (LICs) [3, 5–8]. For example, the implementation of the process of electrosorption of iodine of ACM [17],

$$C^* + I^- - e^- = C^*I, \tag{1}$$

where C* is the surface of the carbon material, with fractional surface coverage θ of the surface of ACM by I ($0 < \theta < 1$) and the electrode potential E, in the system of the prototype of electrochemical energy sources (EES) in charged state

$$Zn|\ 25\%\ ZnI_2|\ C^*I, \tag{2}$$

enables to increase the specific capacitance C_P of ACM to 7376 $F \cdot g^{-1}$

at an average discharge voltage of 1.14 V under galvanostatic conditions of the discharge with a current density i equal to 2.0 $A \cdot g^{-1}$ [17] corresponding to the current-generating process [17]:

$$C^*I + 0.5Zn = C^* + I^- + 0.5Zn^{2+}. \quad (3)$$

In this work, the theoretical data of electrosorption of iodine were determined with the use of Langmuir model and the formula [18]:

$$C_P = (q_I F)(RT)^{-1}\{\theta_I(1 - \theta_I)\}, \quad (4)$$

which indicates the maximum of the pseudocapacitance at $\theta = 0.5$, and the electrode potential of the maximum is considered as equilibrium electrode potential E^0. In an asymmetric design, $Zn \mid C^*I$, C^*I electrode is polarisable with the capacitance C_P, and the Zn (non-polarisable) electrode is chosen so that it has a much higher capacitance (C_{Zn}). In this configuration, where $C_{Zn} >> C_P$, it follows from formula $1/C_T = 1/C_P + 1/C_{Zn}$ that the device capacitance C_T becomes C_P. At the same time, as shown in [17], the polarization of Zn-electrode in an HC system is close to zero, and therefore, the galvanostatic cycle of the whole system of EES represents the polarization $\Delta U = \Delta E$ of NS commercial ACM electrode. In the paper [17], a comparison of the practical and theoretical values of C and W was done; the reversibility of the process of iodine electrosorption enables us to describe the process by means of Langmuir isotherm with weak influence of the interaction of atoms in the adsorption layer.

The aim of this work is to study the influences of kinetic conditions on W, C, and cycling life of the process of iodine electrosorption of NS commercial ACM in the EES system.

2. EXPERIMENT

The 'Norit DLC Supra 30' commercial ACM, ZnI_2 ($\geq 98\%$, Aldrich), and Zn foil (99.999%, Aldrich) were used for our experiments. The NS commercial ACM was microporous activated carbon with highly developed surface area (BET = 1900 $m^2 \cdot g^{-1}$). It was completely described in Ref. [17]. It was produced from natural raw materials [18]. All the chemicals were of analytical grade, and they were used without further purification.

For investigations, there were used film-like electrodes of active mass (m_a) 2–3 mg (S was from 0.18 cm^2 to 0.21 cm^2) with the added binder of 5–10 wt.% of Teflon and 10–20 wt.% of acetylene carbon black or graphite for increase in their electric conductance. The electrodes had been assembled by pressing them to a net of stainless steel. As the electrolyte, 25% ZnI_2 aqueous solution was used.

Electrochemical measurements have been carried out with the use of an AUTOLAB PGSTAT 30 measuring complex made in the Netherlands by 'ECO CHEMIE'. Galvanostatic charge–discharge (GCD) investigations of the prototype of an HC in the system (2) were carried out with the use of measuring two-electrode glass cell with a Zn anode (2 cm^2). Theoretical and experimental of adsorption isotherms are presented in the form of the relation for the electrode polarization $\Delta E = E - E^0$. Experimental values of C_P were determined with the use of discharge voltage steps of $dU = 0.01$ V and corresponding to them differentials $d\theta_I$ according to the following known formula [19]:

$$C_P = q_I(d\theta_I/dU). \quad (5)$$

Here, q_I is the maximal value of NS commercial ACM specific surface charge with iodine atoms ($\theta_{Br} = 0.99$).

C, W, P, θ_I, η of GCD were determined according to the following known formulas:

$$C_c = I_c t_c/m_a \text{ (a)}, \; C_d = I_d t_d/m_a \text{ (b)}, \; \theta_I = C_d/C_{Br,max} \text{ (c)}; \quad (7)$$

$$W = I_d(m_a)^{-1} t_1 \int t^2 U(t)dt \text{ (a)}, \; P = W/t_d \text{ (b)}, \; \eta = C_d/C_c \cdot 100\% \text{ (c)}. \quad (8)$$

Here, C_c, C_d are the specific capacities of charge or discharge respectively; I_d, I_c are the currents of charge and discharge, respectively; t_c, t_d are the times of charge and discharge, respectively; t_1, t_2 are the times of start and finish of discharge, respectively; $C_{I,max} = 1444$ C·g^{-1} is the maximal value of specific gravimetric charge of NS commercial ACM with iodine atoms ($\theta = 0.99$) [17]; $U_{d,max}$ is the maximal value of the discharge voltage; $U_{d,min}$ is the minimal value of the discharge voltage; $\Delta U = U_{c,d,max} - U_{c,d,min}$ denotes the charge–discharge voltage range; m_a is the mass of NS commercial ACM.

3. RESULTS AND DISCUSSION

Galvanostatic cycles (GCs) of NS commercial ACM in the HC system under the conditions of $i_c = i_d$ (i_c and i_d are from 0.5 to 9 A·g^{-1}) are presented in Fig. 1, *a*, *b*, *c*.

The plateau in GC is caused by the processes of pseudocapacitive charge or discharge. For example, the GC presented in Fig. 1, *a* under the conditions of $i_c = i_d$ (i_c and i_d are equal to 0.5 A·g^{-1}) has a plateau of pseudocapacitive charge within the voltage range 1.14–1.25 V (curve *1*) and a plateau of pseudocapacitive discharge within 1.11–1.22 V (curve *1*). On the plateau segment 1.11–1.22 V of the

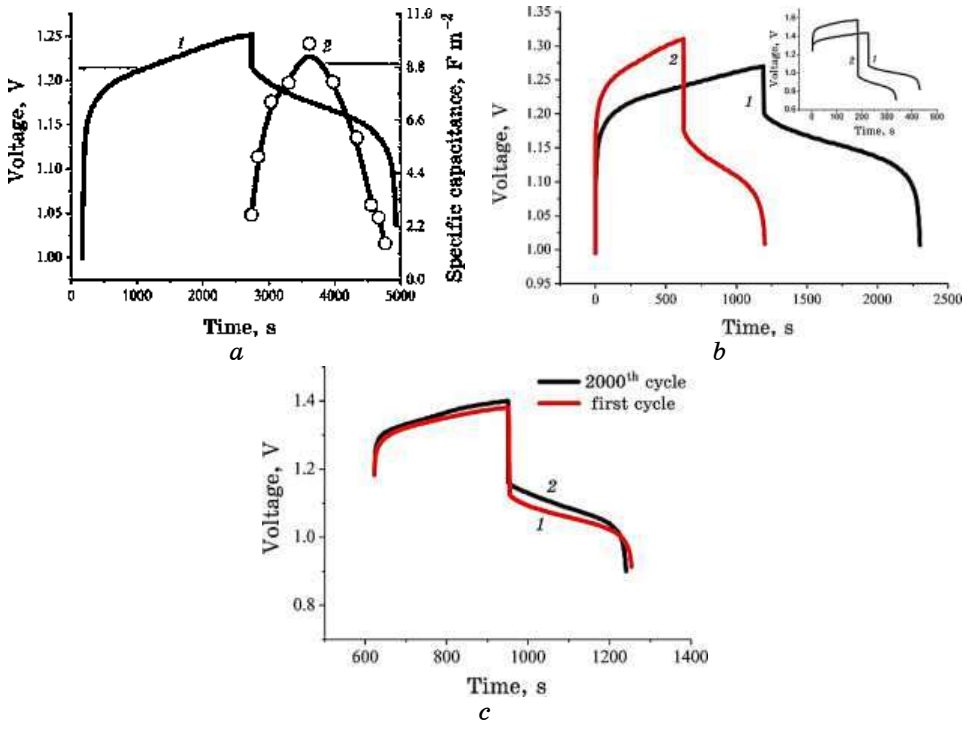

Fig. 1. GCs of NS commercial ACM in the EES system: (*a*) GCD at $i_c = i_d = 0.5$ A·g^{-1} (curve *1*) and dependence of the specific capacitance on the discharge time (curve *2*); (*b*) GCDs at $i_c = i_d = 1$ A·g^{-1} (*1*), at $i_c = i_d = 2$ A·g^{-1} (*2*) and GCDs (inset) at $i_c = i_d = 6$ A·g^{-1} (*1*), and $i_c = i_d = 9$ A·g^{-1} (*2*); (*c*) GCD (*1*—first cycle; *2*—2000th cycle).

discharge curve, high values of C_d, θ_I, $C_{P,d}$, and η were obtained using formulas (5b), (5c), (6b), (7c); they are equal to 1054 C·g^{-1}, 0.73, and 85%, respectively.

According to galvanostatic discharge (GD), using the formula (6d), the dependence of $C_{P,d}$ on discharge time (Fig. 1, *a*, curve *2*) was drawn. It has a maximum of $C_{P,d} = 9.78$ F·m^{-2} at the voltage U^0. This voltage is the voltage of maximum of $C_{P,d}$ and equals to 1.176 V corresponding to the C_d, which is equal to 644 C·g^{-1} ($\theta_I = 0.46$). The polarization of Zn-electrode in an HS system is close to zero, and therefore, the galvanostatic cycle of the whole system represents the ΔE of NS commercial ACM electrode. The polarization of carbon electrode $\Delta E = E - E^0$, according to GD, can be determined by the formula $\Delta E = U - U^0$. The obtained value of the discharge $C_{P,d}$ exceeds the maximal theoretical value of $C_{P,d} = 7.4$ F·m^{-2}, which was calculated in [17]. The increase of $C_{P,d}$ to 9.78 F·m^{-2} is caused by the parameter of interatomic interaction ($g \neq 0$) in the adsorption layer

and by the fact that $\theta_I \neq 0.99$ according to the known formula [19]:

$$C_P = q_I F(RT)^{-1}\theta(1-\theta)\{1+g\theta(1-\theta)\}^{-1}, \quad (8)$$

where $q_I = 0.76$ C·m^{-2} is the maximal value of NS commercial ACM specific surface charge with iodine atoms ($\theta = 0.99$) [17]. Substituting the experimental values $C_{P,d} = 9.78$ F·m^{-2} and $\theta_I = 0.46$ into the formula (8), the practical value of $g = -1$ was calculated. The experimental desorption isotherms (EDI) of iodine as well as the theoretical adsorption isotherm (TAI) of iodine ($g = 0$) [17] were drawn according to GD at the 0.5–9 A·g^{-1}. They are presented in Fig. 2, *a*. Discrepancies between the experimental theoretical isotherms can be accounted for by the influences of $g \neq 0$ and $\theta_I \neq 0.99$. The Frumkin-type isotherm with a parameter g, according to [19], can be represented by the relation

$$E - E^0 = (RT/F)\ln\theta/(1-\theta) + (RT/F)g\theta. \quad (9)$$

As seen from Figure 2, *a*, the increase of θ from 0.73 to 0.87 and that of ΔE from 0.11 V to 0.21 V is caused by the increase in i_d from 0.5 to 9 A·g^{-1}. The corresponding experimental and theoretical ($g = 0$) dependences of $C_{P,d}$ on θ for desorption process, which were drawn according to equation (8), are presented in Fig. 2, *b*. As can be seen from Fig. 2, *b*, the maximum values of the $C_{P,d}$ decreases from 9.8 to 6.3 F·m^{-2} with increase in i_d from 0.5 to 9 A·g^{-1}. The values of g, which were determined using the relation (8), also increase from –0.98 to 0.61 with the increase in i_d (Fig. 2, *b*). Comparison of experimental desorption isotherm (EDI) for $i_d = 9$ A·g^{-1}

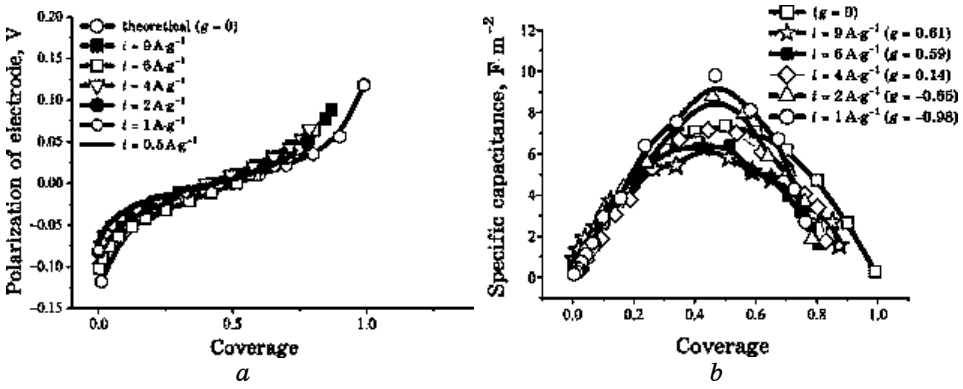

Fig. 2. NS commercial ACM in the EES system: (*a*) TAI ($g = 0$) and EDIs at i_d is equal 0.5–9 A·g^{-1}; (*b*) dependences of the specific capacitance on the fractional surface coverage.

with theoretical adsorption isotherm (TAI) at $g = 0.61$ and further comparison of the latter with TAI at $g = 0$ is shown in Fig. 2, *c*. In Figure 2, *c*, coincidence of the experimental and theoretical ($g = 0.61$) isotherms in the range of θ from 0.1 to 0.6 and the discrepancy between them in other ranges is easily seen; small differences between TAI at $g = 0.61$ and TAI at $g = 0$ can be also seen in the figure. General shape of the GD (Fig. 1, *a*, *b*, *c*) in the narrow segment of voltage ($\Delta E = 0.11–0.21$ V) can be attributed to the process of iodine electrosorption that corresponds to the Frumkin-type adsorption with the small value of interatomic interaction in adsorption layer. Specific energy and specific power are two key factors for evaluating the power applications of EES systems. Using GD data (Fig. 1, *a*, *b*, *c*) with high value of *i* (which increases from 0.5 to 9 $A \cdot g^{-1}$) and formulas (7a), (7b), and (6b), dependences of *W* on *P* (Ragone plot) and of C_d on *P* for NS commercial ACM in the EES system were drawn (Fig. 3, curves *1*, *2*).

They show high values of *P*, C_d and *W*. The increase of *P* from 0.6 to 8 $W \cdot g^{-1}$ leads to increase in C_d from 1060 $C \cdot g^{-1}$ to 1239 $C \cdot g^{-1}$ and to a slight decrease in W from 1240 $J \cdot g^{-1}$ to 1096 $J \cdot g^{-1}$ (Fig. 3, curves *1*, *2*). High values of *C*, *W*, and *P* can be accounted for by peculiarities of the process of iodine electrosorption on the surface of NS commercial ACM. This process provides the great values of $\theta = 0.73–0.87$ at the small values of $\Delta U = 0.11–0.21$ V. An important requirement for EES applications is cycling efficiency or cyclic life. The investigation of cycling efficiency and cycle life for NS commercial ACM electrode in the EES system was based on the data analysis of 2000 GCDs with *i* equal to 4 $A \cdot g^{-1}$ (Fig. 1, *c*). The GCD ($i = 4$ $A \cdot g^{-1}$) presented in Fig. 1, *c* was recorded in the range

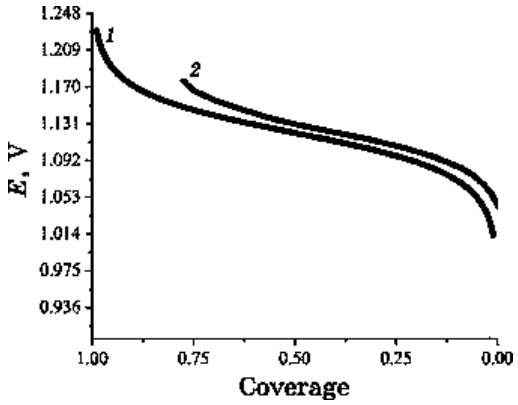

Fig. 3. Dependences of the specific energy on the specific power (curve *1*) and of the specific capacity on the specific power (curve *2*) of NS commercial ACM in the EES system.

1.0–1.38 V for the first cycle and 1.0–1.4 V for the 2000th cycle. Comparison of the 1 and the 2000th cycles shows a decrease in η from 91% in the first cycle to 88% in 2000 cycle, while in the 2000th cycle $C_{P,d}$ slightly decreases to 1148 C·g^{-1}, and W increases to 1264 J·g^{-1} as compared with the 1 cycle 1196 C·g^{-1} and 1227 J·g^{-1}, respectively, at $P = 4.3$ W·g^{-1}. The good cycling performance is ensured here by the optimal surface morphologies of NS commercial ACM and the optimal EES design, which are of huge benefit to facile electrochemical reactions during the long-term cycling.

Theoretical discharge curve was plotted with the use of the measured value of electromotive force of the galvanic couple (11) (EMF = 1.23 V for θ = 0.87) and $\Delta E_{theor} = 0.22$ V (Fig. 4, curve *1*). Theoretical specific energy (W_{theor}) and the experimental one W were calculated with the use of data of Fig. 5 and the use of formula

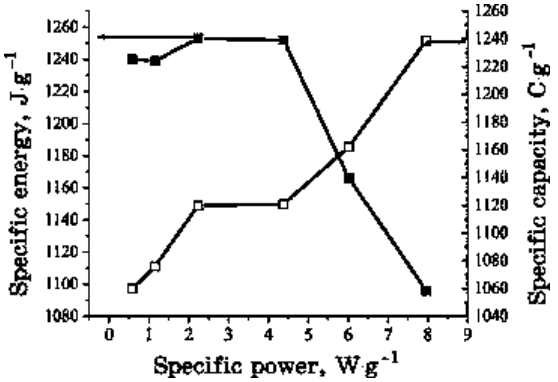

Fig. 4. Theoretical discharge curve ($g = 0.5$) (curve *1*) and experimental GD (*2*) at 2 A·g^{-1}.

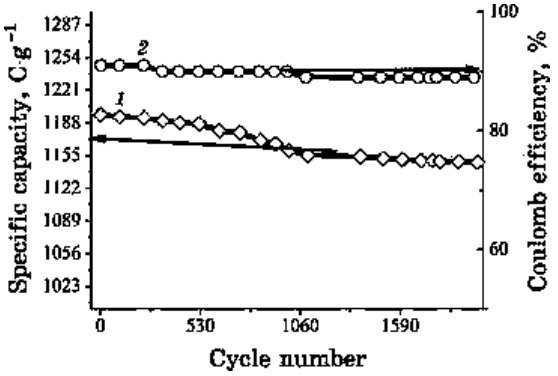

Fig. 5. The specific capacity and Coulombic efficiency as a function of cycle number at a constant current density of 4 A·g^{-1}.

TABLE. Values of g and W_{theor}.

i_d, A·g^{-1}	0.5	1.0	2.0	0	4.0	6.0	9.0
G	–1.0	–0.98	–0.65	0	0.14	0.59	0.61
W_{theor}, J·g^{-1}	1588	1589	1584	1572	1569	1561	1561
W, J·g^{-1}	1240	1239	1253	—	1227	1166	1096

(10a). They are of the values of 1584 J·g^{-1} and 1253 J·g^{-1}, respectively. The obtained experimental value of W is equal to 77% of the theoretical value of W_{theor}. Values of W_{theor}, which were obtained at other i_d, are presented in Table.

The experimentally obtained value $W = 1264$ J·g^{-1} at $P = 4.3$ W·g^{-1} obtained in 2000th cycle of GCD is 80% of the value of $W_{theor} = 1584$ J·g^{-1}.

4. CONCLUSION

Ragone plot for NS commercial ACM in the HC system shows high values of W, C_d and P. The increase in P from 0.6 W·g^{-1} to 8 W·g^{-1} leads to the slight decrease in W from 1198 J·g^{-1} to 1090 J·g^{-1} and to the increase in C_d from 1054 C·g^{-1} ($\theta = 0.73$) to 1256 C·g^{-1}(0.87) and 70–78% discharge of the values W_{theor}. In the 2000th cycle, the high values of W, C_d, P, and η are 1217 J·g^{-1}, 1148 C·g^{-1}, 4.3 W·g^{-1}, 88%, respectively. These high-value characteristics of NS commercial ACM in EES system are due to the high availability of the surface to iodine ($\theta = 0.73$–0.87) as well as due to small positive and negative values of g from –0.98 to 0.61 of the Frumkin process of iodine electrosorption. All of these ones give us the reason to consider the investigated activated material in iodide electrolytes as a prospective electrode for EES construction.

REFERENCES

1. B. E. Conway, *Electrochemical Supercapacitor, Scientific Fundamentals and Technological Applications* (New York: The Kluwer Academic/Plenum: 1999).
2. R. Kotz and M. Carlen, *Electrochim. Acta*, **45**: 2483 (2000).
3. A. G. Pandolfo and A. F. Hollenkamp, *J. Power Sources*, **157**: 1 (2006).
4. *Supercapacitors: Materials, System, and Applications* (Eds. F. Béguin and E. Frackowiak) (Weinheim: Wiley-VCH: 2013).
5. G. Wang, L. Zhang, and J. Zhang, *Chem. Soc. Rev.*, **41**: 787 (2012).
6. L. L. Zhang and X. S. Zhao, *Chem. Soc. Rev.*, **38**: 2520 (2009).
7. Y. Zhang, H. Feng, X. Wu, L. Wang, A. Zhang, T. Xia et al., *Int. J. Hydrogen Energy*, **34**, No. 11: 4889 (2009).

8. J. R. Miller, *Capacitors: Overview. In: Encyclopedia of Electrochemical Power Sources. Vol. 1* (Eds. J. Garche, Ch. K. Dyer, P. T. Moseley, Z. Ogumi, D. A. J. Rand, and B. Scrosati) (Amsterdam: Elsevier B.V.: 2009), p. 587.
9. A. Burke, *Electrochim Acta*, **53**: 1083 (2007).
10. P. Simon and Y. Gogotsi, *Nat. Mater*, **7**: 845 (2008).
11. P. Kurzweil, *Capacitors: Electrochemical Hybrid Capacitors. In: Encyclopedia of Electrochemical Power Sources. Vol. 1* (Eds. J. Garche, Ch. K. Dyer, P. T. Moseley, Z. Ogumi, D. A. J. Rand, and B. Scrosati) (Amsterdam: Elsevier B.V.: 2009), p. 658.
12. L. Feng, Y. Zhu, H. Ding, and C. Ni, *J. Power Sources*, **267**: 430 (2014).
13. S. Faraji and F. N. Ani, *J. Power Sources*, **263**: 338 (2014).
14. M. Chiku, M. Toda, E. Higuchi, and H. Inoue, *J. Power Sources*, **286**: 193 (2015).
15. *Supercapacitors: Materials, System, and Applications* (Eds. F. Béguin and E. Frackowiak) (Weinheim: Wiley-VCH: 2013).
16. P. Simon and A. Burke, *Interface*, **17**, No. 1: 38 (2008).
17. B. P. Bakhmatyuk, *Electrochimica Acta*, **163**: 167 (2015).
18. *Produced by Norit Activated Carbon* (CABOT Inc.) http://www.norit.com/.
19. B. E. Conway, *J. Electrochem. Soc.*, **138**, No. 6: 1539 (1991).